XLI CILAMCE
XLI Ibero-Latin American Congress on Computational Methods in Engineering
16-19 November, 2020 FOZ DO IGUAÇU PARANÁ - BRAZIL

# Use of Third-Order Piston Theory in Panel Flutter Analysis on Composite Laminated Plates with NASTRAN

Victor S. dos Santos[1], Helio A. Pegado[1]

[1]*Dept. of Mechanical Engineering, Universidade Federal de Minas Gerais*
*Av. Pres. Antônio Carlos, 6627 - Pampulha, Belo Horizonte - MG, Brazil*
*victorsantos@ufmg.br, helio@demec.ufmg.br*

**Abstract.** Panel Flutter is an aeroelastic instability of plates and shells of aerospace vehicles. The phenomena have recently grown of interest as the increased efforts to make supersonic and hypersonic flight viable in the upper layers of the atmosphere. Many results are available in the literature using customized programs to study panel flutter with non-linear structural and aerodynamics models. In this work, the third-order Piston Theory is used in the supersonic panel flutter analysis and an evaluation of the NASTRAN capabilities. Later, the mesh convergence study and, subsequentially, the flutter analysis of a metallic and a composite laminated plate is performed. The obtained results show a good agreement with the literature and, therefore, demonstrate the capability of the methodology for the cases developed in this work.

**Keywords:** Panel Flutter, Nastran, Laminated, Composite

## 1 Introduction

Panel Flutter is an aeroelastic instability that brings great challenges and interest in supersonic and hypersonic flight. This instability, which occurs in thin plates and shells of aerospace vehicles, is dynamic and auto-exited by the interaction between elastic, aerodynamic, and inertial forces that generates and keeps the phenomenon. At first, the displacement amplitude of the panel grows exponentially in time, however, the amplitude is frequently limited by the structural non-linearities. This phenomenon is being identified in several aerospace vehicles [1].

This self-excited instability has been extensively studied for decades and involves a system of linear or non-linear differential equations (depending on the approach). Thus, due to the difficulty of obtaining analytical solutions to model the phenomenon with different boundary conditions, the researchers changed the continuous problem into a discrete problem. Firstly, it was employed methods such as Rayleigh-Ritz and Galerkin Method, and later they was discretized with the finite element method (FEM). And, for the study and aeroelastic analysis, the problem was divided into aerodynamic and structural, linear and non-linear, models.

In the previous work by Santos and Pegado [2], an aerodynamic mesh generation and post-processing tool were developed for the aeroelastic flutter analysis in Nastran. In this article a study of the capabilities of MSC.Nastran for aeroelastic modeling and flutter analysis is made. Subsequentially, the mesh convergence analysis is made, followed by a novel analysis of the panel flutter in composite laminated plates, using the aerodynamic third-order Piston Theory. The results obtained are discussed and compared with references from the literature in the following sections.

Nastran has a long development in the aerospace sector since the opening of the original code by the NASA [3], and active use and development. Recent research was made in incorporating Nastran non-linear capabilities in the aeroelastic solutions for flutter [4], and aeroelastic nonlinear trim [5].

This subject still is being debated and researched by the scientific community, with both the use of plates and shells of composites structures [6] [7], and the numerical methods used in his analysis [8] [9].

## 2 Nastran Capabilities

The analysis of aeroelastic stability in the MSC.Nastran is divided into three main modelling components: the aerodynamic model; the interpolation between the structural and aerodynamic elements; and the aeroelastic solution method.

### 2.1 Aerodynamic Modeling

The MSC.Nastran has seven methods for obtaining aerodynamic matrices: The Doublet-Lattice Method (DLM); the ZONA51 or Harmonic Gradient Method (HGM); the Constant Pressure Method (CPM); the DLM with wing-fuselage interference; the Mach Box Method (MBM); the Strip Theory; and the Piston Theory. All methods support non-stationary flow, differing about the applied aerodynamic theory [10, p. 17].

A summary of the main characteristics of the supersonic methods are shown in Table 1, describing which aerodynamic theory was used, which utilized discretization method, and in which Mach number regime the method fits [11].

Table 1. Resume of the aerodynamic modeling techniques.

| **Element** | **Method** | **Aerodynamic Theory** | **Discretization** | **Mach Range** |
|---|---|---|---|---|
| CAERO1 | HGM | Acceleration Potential | *Boxes* | $1.1 < M < 3.0$ |
| CAERO1 | CPM | Acceleration Potential | *Boxes* | $1.1 < M < 3.0$ |
| CAERO3 | MBM | Velocity Potential | *Boxes* | $1.2 < M < 3.0$ |
| CAERO5 | *Piston Theory* | $3^{\text{rd}}$ Order Piston Theory | *Strips* | $2.5 < M < 7.0$ |

The potential aerodynamic theories, as all lifting line theories, do not take into account the thickness of the aerodynamic profile, which may induce some modeling errors since the thickness has an effect of reducing the flutter speed [11, p. 331]. This does not occur in the Piston Theory method, which allows the correction of thickness.

The Boxes discretization is arranged as a planar grid of rectangular or triangular elements, that has aerodynamic interaction between the boxes and multiple elements, except on MBM, that only has interaction within the element surface. In counter part, the Strips discretization uses coplanar spanwise strips, that has no aerodynamic interaction between each strip, or between multiple elements.

Two specific differences are notable in the implementation: the CPM method does not provide the use of triangular elements; and the MBM method requires the user to define the geometry of the aerodynamic surface to then compute the aerodynamic mesh.

MSC.Nastran allows the modeling of control surfaces, corrections for sweep angle, compressibility, symmetry, among other properties. Such possibilities will not be discussed as they are outside the scope of this work.

There are also restrictions of geometric nature: every aerodynamic element must be aligned with the wind axis (x-axis of the aerodynamic coordinate system), which leads to some difficulties in modeling, for example, the incidence of wings and angle of attack (AoA), creating the need for aerodynamic correction matrices; and in Strip discretization methods, the element's chord line must remain rigid, that is, without deformations along its chord line; on CAERO1 elements is desirable that the chord of each box is less than $0.08V/f$, being $f$ the greatest frequency of interest and $V$ the lowest velocity of interest.

Regarding the numerical implementation of the methods, it is notable that the DLM and HGM methods need to compute the inverse of the aerodynamic influence coefficients matrix (AIC). Since it is not directly computed, a matrix decomposition and substitution process is needed to obtain it. In the other methods, there are direct solutions for A, and no need for inverting matrix techniques, which reduces the computational cost of the analysis [12, p. 45-57].

As final remarks, the aerodynamic Piston Theory is most suitable for the Panel Flutter analysis at high Mach numbers, since there is better agreement than the MBM [12, p. 68-74], and the modeling is computationally less expensive than the HGM that requires the use of two additional aerodynamic elements side by side with the main panel, so the Mach cone does not interfere on the panel region [13].

The downsize of using the Piston Theory is the need of parallel strip elements and the use of beam splines for each element, increasing the number of NASTRAN cards needed. This downsize is diminished with pre-prossesing tools such as the method developed by Santos and Pegado [2], tools like the pyNastran package by Doyle [14] or commercial CAE (Computer-Aided Engineering) tools.

### 2.2 Aero-Structure Interpolation

To obtain the coupled aerodynamic and structural matrices, it is necessary to interpolate nodal displacements and nodal forces between the aerodynamic and structural elements. For this purpose, the MSC.Nastran provides five interpolation methods, totaling ten solution options. However, we can cluster two groups of options that are most relevant to the panel flutter problem: The Surface Splines; and the Linear Splines.

The Surface Spline is based on the theory of flat plates, obtaining a function of two variables to model the forces and displacements, ideal for low aspect-ratio models. The Linear Splines are based on beam theory, ideal for high aspect-ratio models.

### 2.3 Aeroelastic Solution Methods

MSC.Nastran provides six methods of aeroelastic solution for flutter: the American K-method; the KE-method; the English PK-method; the PKNL-method; the PKS-method; and the PKNLS method. A summary of the characteristics of each method is shown in Table 2.

Table 2. Resumo de características dos métodos de solução aeroelástica.

| Method | Description | Input | Output |
|---|---|---|---|
| K | Classic American iterative method | Sets of $M$, $k$ and $\rho$ | $V$, $g$ and $f$. |
| KE | *K-method* with eigenvalue solution only | Sets of $M$, $k$ and $\rho$ | $V$, $g$ and $f$. |
| PK | Classic British iterative method. | Combinations of $V$, $M$ and $\rho$ | $V$, $\gamma$ and $f$. |
| PKS | *PK-method* derived. "Sweeps" around $k$ values | Combinations of $V$, $M$ and $\rho$ | $V$, $\gamma$ and $f$. |
| PKNL | *PK-method* derived | Sets of $V$, $M$ and $\rho$ | $V$, $\gamma$ and $f$. |
| PKNLS | *PKS-method* derived | Sets of $V$, $M$ and $\rho$ | $V$, $\gamma$ and $f$. |

In the PK derived methods, there is the direct input of the velocities, which is preferable to the type K derived methods, which requires a process of ordering the eigenvalue solution and computation the velocities. In the no-loop (or non-iterative) methods (i.e. NL methods), there is no possibility of iteration error due to improper loop iteration. And, according to Rodden and Johnson [13], the damping parameter $\gamma$ in PK type methods is more physically significant than the $g$ parameter in type K methods.

All the PK derived methods should yield the same overall result if configured properly. The K derived methods should agree with the PK's results just on the critical values. The use of which is a choice of preference on how the inputs and outputs are handled.

## 3 Procedures

The analysis developed in this work was carried out with the strip discretization of the Third-Order Piston Theory (CAERO5), with parallel elements, using the PK-method, and interpolation with the structure by Beam Splines.

It was used the code previous developed by Santos and Pegado [2], now using the pyNastran package, and adding the capability to analyze panel flutter with CAERO1 elements and surface interpolation (SPLINE1) for comparative results.

### 3.1 Mesh Convergence Study

For the mesh convergence study, it was adopted a well-known model in the panel flutter literature, a simply supported rectangular plate, of dimensions: 300mm of length ($a$), 300mm of width ($b$), and 1,5 mm of thickness ($t$). The material adopted was aluminum.

A Mach number ($M$) of 3 was adopted, reference density at sea level (ISA), and reference chord equal to the length of the plate. It was used a speed range between $822\,\mathrm{m/s}$ and $1066\,\mathrm{m/s}$, which, given a Mach value, corresponds to the maximum and minimum speed of sound within the standard atmosphere.

The material properties used in the analysis were: modulus of elasticity ($E$) of $71.7\,\mathrm{GPa}$; shear modulus ($G$) of $26.9\,\mathrm{GPa}$; Poisson's ratio ($\nu$) of $0.33$; and density ($\rho_m$) of $2.81\,\mathrm{g/cm^3}$. For comparative purposes, the values of the two parameters were computed: the dimensionless dynamic pressure ($\lambda$), given by

$$\lambda = \frac{2\bar{q}a^3}{\beta D}, \tag{1}$$

where $\bar{q}$ is the dynamic pressure, and $\beta$ is the dimensionless value given by

$$\beta = \sqrt{M^2 - 1}, \tag{2}$$

and $D$ is the flexural rigidity of the plate given by

$$D = \frac{Et^3}{12(1 - \nu^2)}; \tag{3}$$

and the densities ratio by the Mach number $(\mu/M)$ , where the densities ratio $(\mu)$ is given by

$$\mu = \frac{\rho_a a}{\rho_m t}, \tag{4}$$

where $\rho_a$ is the undisturbed air density.

The first two theoretical vibration frequencies for the plate were also calculated analytically using the classic thin plate theory.

For the initial mesh size, 10x10 aerodynamic and structural elements were adopted, based on the HA145HA model. $N$ multiples of this mesh were then analyzed.

It is also possible to analyze configurations in which the aerodynamic and structural mesh sizes are not the same. However, it falls into some issues.

In the case where the aerodynamic mesh is smaller than the structural one, more than two structural nodes will belong to the region of the aerodynamic elements, in the same y coordinate. If all nodes were selected, it would have the development of a singular matrix, which makes the solution unfeasible.

An alternative would be to use values greater than zero for the parameter $D_z$ of displacement attachment, which means that the interpolation does not necessarily go through all designated points, acting like springs were attached to the nodes. However, this alternative violates the rigid chord hypothesis of the piston theory and leads to unsatisfactory results.

Also, if only a portion of the nodes were selected, there would be a loss of physical meaning, since the displacement of the reminiscent nodes would not imply a change in the aerodynamic nodes.

For the case in which the aerodynamic mesh is larger than the structural one, there is a limitation of it being twice the structural mesh size. This is given the fact that in any other configuration there would be aerodynamic panels without corresponding structural nodes, or ambiguous relations. Even if they were connected to the adjacent structural nodes, it would not improve the quality of the model since their displacements would be equal to those of the neighbor panels.

In cases of refinement of the aerodynamic mesh longitudinally (i.e. y-direction), there is no improvement in the result, since that this Piston Theory is discretized in strips, and there is no aerodynamic interaction between them. Besides, for square plates, the use of non-symmetric structural mesh sizes, that is, a different number of elements in the longitudinal and lateral directions, is not appropriate since it can produce errors in the solution of the modal analysis.

The Table 3 show the values of critical dimensionless dynamic pressure $(\lambda_c)$, estimated degrees of freedom of the model (DOF), and the first two computed vibration frequencies.

The errors compared with the literature are shown in Table 4. The parameters $\beta a/b = 2.83$ and $\mu/M = 0.0291$ were used for interpolating the values of Hedgepeth [15] and Pegado [16], respectively. The analytical values of the frequencies are $f_1 = 80.88\,\mathrm{Hz}$ and $f_2 = 202.20\,\mathrm{Hz}$.

Satisfactory results were obtained with the 20x20 mesh in the mesh convergence analysis, with an error of less than $1\,\%$ to the reference value of Pegado [16]. For the values found by Hedgepeth [15, Table 2] the error is less than $5\,\%$.

For meshes with larger numbers of elements, there was relatively little accuracy gain, while there was a significant increase in the number of degrees of freedom and consequently an increase in computational cost.

Table 3. Mesh convergence study results.

| Mesh Size | $\lambda_c$ | DOF | $f_1$ (Hz) | $f_2$ (Hz) |
|---|---|---|---|---|
| 10x10 | 524.34 | 606 | 79.80 | 198.50 |
| 20x20 | 518.67 | 2406 | 80.48 | 200.92 |
| 30x30 | 517.81 | 5406 | 80.64 | 201.49 |
| 40x40 | 517.07 | 9606 | 80.69 | 201.70 |

Table 4. Mesh convergence study comparative results.

| Mesh Size | Error | | | |
|---|---|---|---|---|
| | $\lambda_c$ Hedgepeth [15] | $\lambda_c$ Pegado [16] | $f_1$ | $f_2$ |
| 10x10 | 5.67 % | 1.78 % | −1.34 % | −1.83 % |
| 20x20 | 4.53 % | 0.68 % | −0.50 % | −0.64 % |
| 30x30 | 4.36 % | 0.52 % | −0.30 % | −0.35 % |
| 40x40 | 4.21 % | 0.37 % | −0.24 % | −0.25 % |

It is possible to infer that there is a correlation between the precision of the frequencies of the first modes of vibration with the precision of the $\lambda_c$ value. That is expected, since, the coupling of the first two modes generates the most critical flutter condition, and therefore, the precision with which the first modes are represented in the FEM model directly impacts the result.

Therefore, the use of a 20x20 mesh was found to be the most suitable, as it provides good accuracy with a relatively low computational cost. It can be suggested that in configurations where $a \neq b$, or asymmetry exists, other mesh values should be used (e.g. keeping the aspect ratio of the element adequate), but that a minimum of 20 elements be kept in each dimension.

### 3.2 Laminated Composite Plate Analysis

The model adopted was of the same geometry, boundary conditions, and flow properties as the convergence study model, besides a value of $M = 2$ and the appropriate speed range. The material used for the composite laminate was Glass-Epoxy (GFRP) with properties described in Table 5. The layers were arranged according to the methodology described by Sawyer [17], as in Table 6. The orientation angle ($\theta$) for the laminate layers ranges from 0 to 90 with a step of 10. The choices of material properties and layering of the layers were arbitrarily chosen for comparison with the reference methodology.

Table 5. GFRP mechanical properties.

| $E_1$ (GPa) | $E_2$ (GPa) | $G_{12}$ (GPa) | $\nu$ | $\rho_m$ (g/cm$^3$) |
|---|---|---|---|---|
| 54 | 18 | 7.2 | 0.3 | 2.6 |

## 4 Results & Discussions

Using the 20x20 mesh, the analysis was performed, obtaining the values of

$$\lambda^* = \frac{2\bar{q}a^3}{\beta D_{11}} \tag{5}$$

Table 6. Ply sheets configuration.

| Sheet | Orientation (°) | Thickness (mm) |
|---|---|---|
| 1 | $\theta$ | 0.5 |
| 2 | $-\theta$ | 0.5 |
| 3 | $-\theta$ | 0.5 |
| 4 | $\theta$ | 0.5 |

as a function of $\theta$. Then it was compared with the result obtained by Sawyer [17], as shown in Figure 1. The parameter $D_{11}$ is similar to the previously used, however, as the flexural rigidity of the plate becomes a matrix, due to the nature of the composite material, the parameter $D_{11}$ is used with $\theta = 0°$ as a reference value. The value of $D_{11}$ can be easily computed in most software that supports laminate analysis.

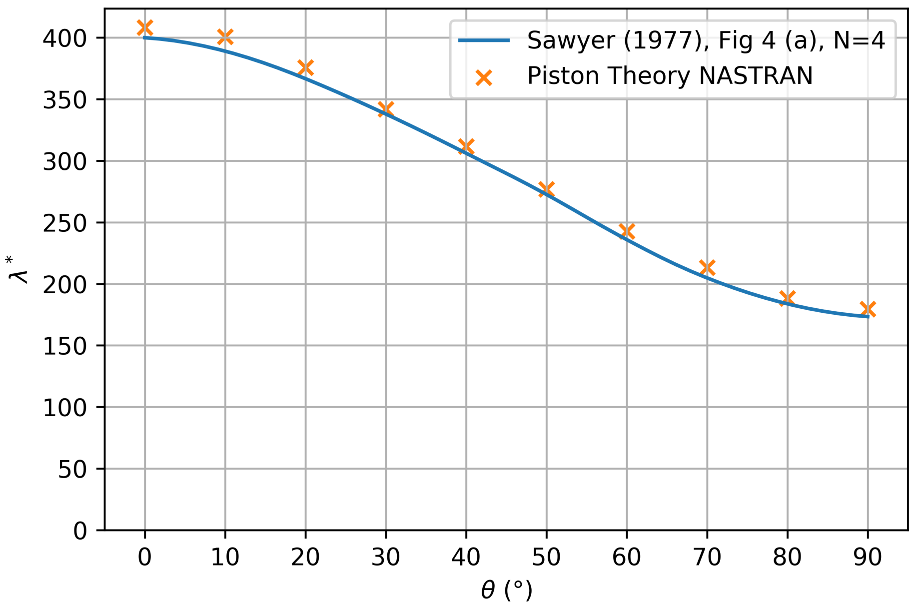


Figure 1. Values of critical dimensionless dynamic pressure as function of ply sheets orientation.

The methodology applied to the composite panel problem agrees to the reference results, observing the same trend and with an error of less than $5\,\%$, however, the results converge from above, which indicates a non-conservative trend of the model, already been reported by [13].

## 5 Conclusion

In this work, the aeroelastic stability analysis with the FEM and the third-order Piston Theory of a laminated composite plate was performed. A study of the NASTRAN capabilities was made, indicating the benefits and downsides of each modeling solution. The desired mesh value was obtained from the mesh convergence study. And, finally, the obtained results agreed to those found in the literature, however, all cases were shown to be non-conservative.

As demonstrated by the applicability of the methodology, it is possible to analyze geometrically similar structures, with different materials (e.g. composites), and adjacent structures (e.g. reinforcers), without modeling difficulties. However, the analysis in cases of non-flat geometry (e.g. curved panels, shells) may lead to other problems and requires more development of the methodology.

Future works may implement the use of NASTRAN's geometric non-linear solution (i.e. large deformations), heat transference analysis, aeroservoelastic analysis, and the use in optimization problems for aeroelastic tailoring.

**Acknowledgements.**

**Authorship statement.** The authors hereby confirm that they are the sole liable persons responsible for the authorship of this work, and that all material that has been herein included as part of the present paper is either the property (and authorship) of the authors, or has the permission of the owners to be included here.

## References

[1] Pegado, H. d. A., 2006. Flutter de painéis: mais um desafio no vôo supersônico. *Exacta*, vol. 4, n. 2, pp. 235–245. Publisher: Universidade Nove de Julho.

[2] Santos, V. & Pegado, H. D. A., 2019. Finite Element Method Modeling of Supersonic Panel Flutter with Piston Theory. In *Proceedings of the 25th International Congress of Mechanical Engineering*. ABCM.

[3] MacNeal, R. H., 1974. Some organizational aspects of NASTRAN. *Nuclear Engineering and Design*, vol. 29, n. 2, pp. 254–265.

[4] Anand, H., 2019. Nonlinear Aeroelastic Analysis of a High Aspect Ratio Wing in NASTRAN. pp. 64.

[5] Riso, C., Vincenzo, F. G. D., Ritter, M., Cesnik, C. E. S., & Mastroddi, F., 2017. A FEM-BASED APPROACH FOR NONLINEAR AEROELASTIC TRIM OF HIGHLY FLEXIBLE AIRCRAFT. pp. 18.

[6] Guimarães, T. A. M., Castro, S. G. P., Cesnik, C. E. S., & Rade, D. A., 2019. Supersonic Flutter and Buckling Optimization of Tow-Steered Composite Plates. *AIAA Journal*, vol. 57, n. 1, pp. 397–407. _eprint: https://doi.org/10.2514/1.J057282.

[7] Akhavan, H. & Ribeiro, P., 2018. Aeroelasticity of composite plates with curvilinear fibres in supersonic flow. *Composite Structures*, vol. 194, pp. 335–344.

[8] Vincenzo, F. G. D., 2019. A NEW OPEN FLUID-STRUCTURE INTERFACE FOR STEADY AND UNSTEADY NONLINEAR SIMULATIONS. In *International Forum on Aeroelasticity and Structural Dynamics IFASD 2019*, pp. 25, Savannah, Georgia, USA.

[9] Modaress-Aval, A. H., Bakhtiari-Nejad, F., Dowell, E. H., Shahverdi, H., Rostami, H., & Peters, D., 2020. Aeroelastic analysis of cantilever plates using Peters' aerodynamic model, and the influence of choosing beam or plate theories as the structural model. *Journal of Fluids and Structures*, vol. 96, pp. 103010.

[10] Patran/Nastran, M., 2019. *Aeroelastic Analysis User's Guide*. MSC Software Corporation.

[11] Liu, D. D., Chen, P. C., Yao, Z. X., & Sarhaddi, D., 1996. Recent advances in lifting surface methods. *The Aeronautical Journal*, vol. 100, n. 998, pp. 327–340. Publisher: Cambridge University Press.

[12] Rodden, W. P., 1979. *Aeroelastic addition to NASTRAN*. Washington, D.C. :.

[13] Rodden, W. P. & Johnson, E. H., 1994. *MSC/NASTRAN aeroelastic analysis: user's guide; Version 68*. MacNeal-Schwendler Corporation.

[14] Doyle, S., 2020. SteveDoyle2/pyNastran. original-date: 2015-03-12T18:50:27Z.

[15] Hedgepeth, J. M., 1957. Flutter of Rectangular Simply Supported Panels at High Supersonic Speeds. *Journal of the Aeronautical Sciences*, vol. 24, n. 8, pp. 563–573.

[16] Pegado, H. d. A., 2003. Método de Perturbações no Estudo de Não-linearidades na Aeroelasticidade de Painéis em Regime supersônico. *91f.: sn*.

[17] Sawyer, J. W., 1977. Flutter and Buckling of General Laminated Plates. *Journal of Aircraft*, vol. 14, n. 4, pp. 387–393.